Acta Pharmacologica Sinica

www.nature.com/aps

ARTICLE

Rg1 improves LPS-induced Parkinsonian symptoms in mice via inhibition of NF-κB signaling and modulation of M1/M2 polarization

Jia-qi Liu[1,2], Ming Zhao[3], Zhao Zhang[1], Li-yuan Cui[1], Xin Zhou[1], Wei Zhang[4], Shi-feng Chu[1], Da-yong Zhang[2] and Nai-hong Chen[1]

Ginsenoside Rg1 is one of the most active ingredients in ginseng, which has been reported to protect dopaminergic neurons and improve behavioral defects in MPTP model, 6-OHDA model and rotenone model. However, it is unclear whether Rg1 exerted neuroprotection in LPS-induced sub-acute PD model. In this study, we investigated the neuroprotective effect of Rg1 in the sub-acute PD mouse model and explored the related mechanisms. Rg1 (10, 20, 40 mg·kg^{-1}·d^{-1}) was orally administered to mice for 18 days. A sub-acute PD model was established in the mice through LPS microinjection into the substantia nigra (SN) from D8 to D13. We found that Rg1 administration dose-dependently inhibited LPS-induced damage of dopaminergic neurons and activation of glial cells in the substantia nigra pars compacta (SNpc). The neuroprotective effects of Rg1 were associated with the reduction of pro-inflammatory cytokines and the improvement of anti-inflammatory cytokines and neurotrophin in the midbrain. Rg1 shifted the polarization of microglia towards the M2 phenotype from M1, evidenced by decreased M1 markers (inducible NO synthase, CD16, etc.) and increased M2 markers (arginase 1 (Arg1), CD206, etc) in the midbrain. Furthermore, Rg1 administration markedly inhibited nuclear translocation of NF-κB in midbrain microglia. In conclusion, Rg1 protects PD mice induced by continuous LPS injection by inhibiting the nuclear entry of NF-κB and regulating the polarization balance of microglia, shedding new light on a disease-modifying therapy of PD.

Keywords: Parkinson's disease; ginsenoside Rg1; neuroinflammation; lipopolysaccharide; microglia polarization; NF-κB

Acta Pharmacologica Sinica (2020) 41:523–534; https://doi.org/10.1038/s41401-020-0358-x

INTRODUCTION

Parkinson's disease (PD) is a common neurodegenerative and disabling disease in middle and old age, with substantia nigra (SN) as the main lesion site. The clinical symptoms of PD patients include motor symptoms and nonmotor symptoms. The characteristic manifestations of motor symptoms are tremor and slowness of movement [1]. The main pathological features are progressive loss of dopaminergic neurons in the SN and the presence of Lewy bodies (a-synuclein as the main component) in the remaining neurons in the substantia nigra compact (SNC). There are many pathogenesis mechanisms of PD, among which the inflammatory mechanism (mainly the rapid activation of microglia) is closely related to the pathogenesis of PD [2]. This has attracted extensive attention from researchers.

Currently, the lipopolysaccharide (LPS) animal model is the most universal model for studying the relationship between neuroinflammation and PD [3–5]. There are many ways to establish LPS animal models: intraperitoneal injection, intracerebroventricular injections and nasal inhalation, among others. The LPS intraperitoneal injection model has the disadvantage that LPS cannot disrupt the permeability of the blood–brain barrier (BBB) [6]. Intracerebroventricular injection does not specifically stimulate microglia in the SN, lacking specificity. Although nasal inhalation avoids the BBB, the modeling cycle is longer [7]. Therefore, we established a subacute PD model by injecting LPS for five consecutive days into the SN. This model could specifically and directly induce microglial activation in the SN, avoiding the interference of microglial activation in specific brain regions related to other nervous system diseases. Moreover, it took less time to establish the model, with less loss of manpower, material, and financial resources.

One of the most prominent features in PD animal models is neuroinflammation mediated by microglia. Increasing evidence indicates that microglial activation in the brains of PD animals is heterogeneous and can be classified into the M1 phenotype and M2 phenotype. Pisanu et al. and Eugene Bok et al. further observed that the process of dopaminergic degeneration was associated with the gradual increase in M1 polarization over M2 polarization in microglia in chronic PD mice [8, 9]. In normal and PD mice, both M1 and M2 polarized phenotypes are observed, but in PD mice there are more M1 phenotype microglia than M2 phenotype. It has been reported that some transcriptional regulators could turn on the core switches of M1 and M2 genes to promote polarization. NF-κB is one of the transcription factors

[1]State Key Laboratory of Bioactive Substances and Functions of Natural Medicines, Institute of Materia Medica and Neuroscience Center, Chinese Academy of Medical Sciences and Peking Union Medical College, Beijing 100050, China; [2]China Pharmaceutical University, Nanjing 210009, China; [3]Beijing Hospital, Beijing 100730, China and [4]Institute of Chinese Integrative Medicine Hebei Medical University, Shijiazhuang 050017, China
Correspondence: Da-yong Zhang (cpuzdy@163.com) or Nai-hong Chen (chennh@imm.ac.cn)

Received: 25 September 2019 Accepted: 1 January 2020
Published online: 18 March 2020

that causes M1 polarization of microglia [10]. NF-κB also plays an important regulatory role in the inflammatory response. After activation, NF-κB enters the nucleus, binds with a variety of cellular inflammatory factor promoter region κB sequences and participates in the transcription of inflammatory mediators (IL-2, IL-6, TNF-a, etc.) and NO synthase. Mogi et al. found clear activation of NF-κB in the SN neurons in brain slices of PD patients [11]. Daily et al. also reported that nuclear NF-κB-positive neurons in the brains of PD patients were 70 times higher than those in the normal control group [12]. These results indicate that the intranuclear translocation of NF-κB is involved in the pathophysiological process of PD.

PD has a high prevalence and a long course, so it is of great significance to study the treatment and related mechanisms of this disease. Ginsenoside Rg1 is extracted from the dried roots of *Panax ginseng* C.A. Meyer (Araliaceae) and has significant pharmacological activities [13]. At present, a large number of studies have shown that Rg1 plays an anti-inflammatory role in neurodegenerative diseases [14, 15]. Reale et al. also found that Rg1 has a protective effect on dopaminergic neurons in PD models induced by neurotoxins such as MPTP, 6-OHDA and rotenone [16–19]. However, it is still unclear what the mechanism of action of Rg1 is in subacute PD mice injected multiple times with LPS via SN and whether Rg1 exerts its expected protective effect.

In this study, we examined whether Rg1 could improve PD-like symptoms induced by multiple injections of LPS in the SN by exerting a neuroprotective effect. In addition, we observed the effects of Rg1 on proinflammatory and anti-inflammatory cytokines in the LPS-lesioned SN. Finally, we demonstrate that Rg1 inhibits M1 phenotypic polarization of microglia by inhibiting nuclear translocation of NF-κB and skews it toward M2 phenotype polarization.

MATERIALS AND METHODS

Reagents

Lipopolysaccharide and glycerol were purchased from Sigma-Aldrich (St. Louis, MO, USA); saline was obtained from Sichuan Kelun Pharmaceutical Co., Ltd. (Chengdu, China); Rg1 (HPLC ≥ 98%) was obtained from Shanghai Yuanye Biotechnology Co., Ltd. (Shanghai, China); and levodopa (L-Dopa) tablets were obtained from Beijing Shuguang Pharmaceutical Co. LTD (Beijing, China). Unless otherwise specified, all other chemicals and reagents used were of analytical grade.

Animals

In total, 126 male pathogen-free C57BL/6 mice, weighing 25–30 g, aged 9–10 weeks, provided by the Experimental Animal Center of the Chinese Academy of Medical Sciences (Beijing, China), were used for the preparation of the subacute PD model. They were raised on a 12 h light/dark cycle with ad libitum access to food and water and were housed in clean cages under conditions of 22 ± 1 °C room temperature and 55% ± 5% relative humidity. All animal protocols followed the guidelines established by the National Institutes of Health and were approved by the Animal Care and Use Committee of the Peking Union Medical College and Chinese Academy of Medical Sciences.

Surgical operations and LPS treatment

The LPS-induced subacute PD mouse model was prepared as previously described with modifications (Fig. 1) [20]. After seven days of acclimatization, the mice were pretrained in three tests that included the rotarod experiment, pole test and grip test (excluding mice with poor motor coordination). Mice remember the acquired tasks on the 14th day of the experiment.

According to the different treatments, the mice were randomly divided into seven experimental groups used after

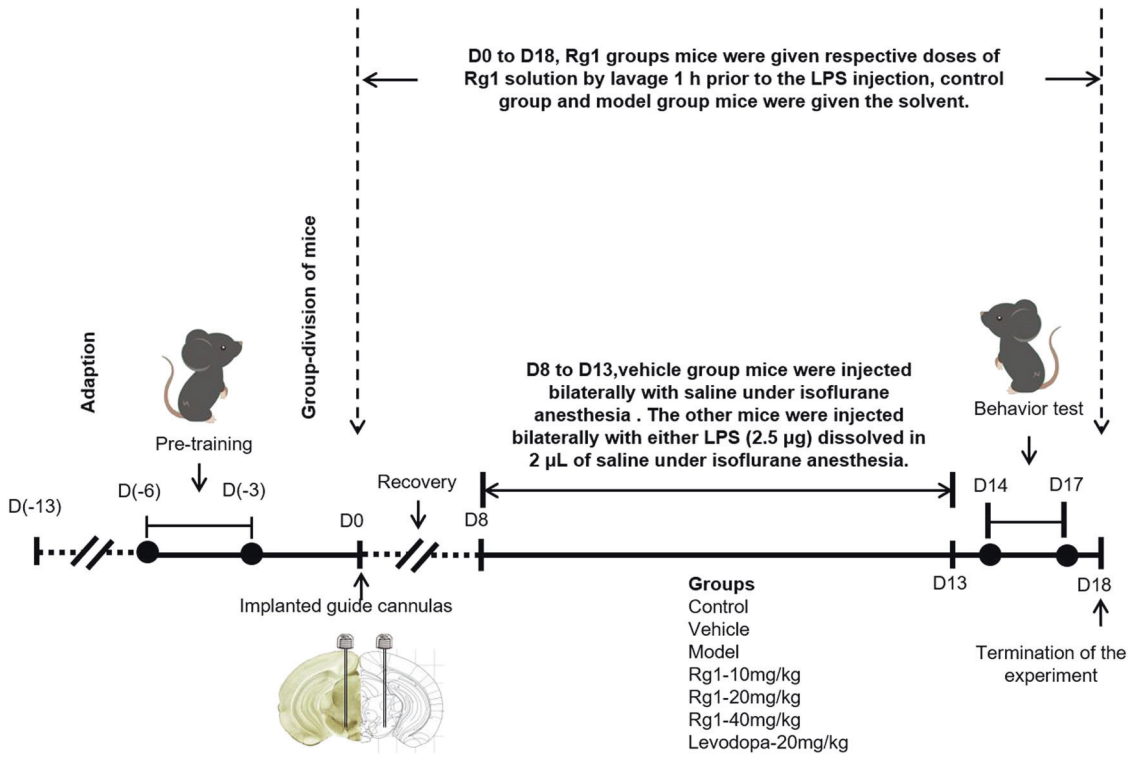

Fig. 1 Scheme of the experiment procedure. After seven days of acclimatization, the mice were pretrained in three behavior tests. The mice were then randomly divided into seven experimental groups. One hour prior to the guide cannula implantation, the mice of Rg1 treatment groups and levodopa group were orally administered Rg1 or levodopa, respectively, from D0 to D18. The mice, except the control group, were implanted with two-sided hole guide cannulas. Eight days after surgery, the mice implanted with cannulas were injected bilaterally with LPS or saline, from D8 to D13. From D14 to D17, a series of behavior tests were conducted. On D18, all mice were sacrificed for further study

pretraining. Group I: Control group; Group II: Vehicle group; Group III: Model group; Group IV: Rg1 (10 mg/kg) group; Group V: Rg1 (20 mg/kg) group; Group VI: Rg1 (40 mg/kg) group; and Group VII: Levodopa (20 mg/kg) group. All groups of mice received the following corresponding treatments accordingly.

One hour prior to the guide cannula implantation, mice in group IV–VII were orally administered 10, 20, or 40 mg/kg Rg1 or 20 mg/kg levodopa, respectively, from D0 to D18. Mice in groups I–III were orally administered solvent water. Thereafter, mice in groups II–VII were implanted with two-sided hole guide cannulas. The cannulas were fixed to the skull with dental cement. The mice in the control group had no treatment. Eight days after surgery, the group III-VII mice were injected bilaterally with either LPS (2.5 μg) dissolved in 2 μL of saline into both sides of the substantia nigra pars reticulata (SNR) (3.28 mm posterior, 1.50 mm lateral and 4.60 mm ventral to the bregma), from D8 to D13. In group II, solvent saline was injected into both sides of the SNR. The injection was conducted over a period of 5 min and controlled by a motorized microinjection pump. After the injection, the needle was kept in place for 3 min to prevent solvent spillage. All surgically treated mice were anesthetized with 2% isoflurane by mask and maintained with 1.5% isoflurane. The mice were placed on a heating pad to maintain the body temperature and for recovery after surgery.

Behavior testing and mortality

From D14 to D17, a series of behavior tests were conducted to observe the behavioral changes in all groups. All behavior tests were performed under normal mouse room light conditions and in quiet experimental sites. The rotarod test was performed on D15, the pole test was performed on D16 and the basic grip test was performed on D17.

Rotarod test

Rotarod testing requires mice to maintain balance and continuous movement on the rollers, which is widely used to detect the coordination of movement in mice. The test method has been described previously [17]. The rotarod apparatus (IITC Life Science, Woodland Hills, CA, USA) was programmed to rotate with linearly increasing speed from 5 rpm to 30 rpm in 5 min. The latency time of mice on the rotarod apparatus was recorded. Then, the next test was conducted after a 30 min interval. The average value after three measurements was recorded.

Pole test

The pole test was performed as previously described by Ogawa with minor modifications [21]. The pole equipment consisted of a homemade straight wooden pole (50 cm high and 1 cm diameter), which was wrapped with gauze to prevent mice from slipping. The bottom of the wooden pole was placed in a cage, covered with bedding to protect the mice from injury, and the top was fixed with a wooden ball. The recorded data were the time it took for mice to crawl from the top to the bottom of the pole. The interval between the two tests was 30 min to ensure the recovery of physical strength in mice. Each mouse was tested three times and averaged.

Grip strength test

The grip strength test is used to evaluate the effect of drugs on grip strength in mice. The apparatus was a YLS-13A grip strength meter with a mouse grip plate. During the experiment, the mice were placed on the grip strength meter. Next, the tail of the mouse was caught and pulled back in a straight line, recording the grip data and printing it. Each mouse was tested six times and averaged.

Mortality surveillance

We recorded the number of dead mice in every group before each injection.

Tissue processing

On D18, all mice were sacrificed by dislocating the cervical vertebrae or perfusion after anesthesia for further study. Six mice in each group were anesthetized by chloral hydrate (400 mg/kg, ip) upon termination of the experiment. After a few minutes, the anesthetized mice were fixed on the operating table in a supine position. Next, the thoracic cavity of the mice was carefully opened, and the ribs were quickly cut. Then, the diaphragm was cut off to adequately expose the heart. The injection needle filled with 0.1 M phosphate-buffered saline (PBS) was inserted into the mouse left ventricle to flush blood from the blood vessels. After the liver turned white, the mice were fixed with 4% paraformaldehyde (PFA). After perfusion, the brains were removed and stored in 4% PFA. Before sectioning, the brain tissues were successively dehydrated using a 10%, 20%, and 30% sucrose PFA gradient. After cryoprotection, the striatum or SN of the brain was cut into 20-μm sections for subsequent analysis. After anesthesia, the rest of the mice in each group were sacrificed, and the brains were collected on ice plates. The middle brain tissue and striatum tissue were isolated and stored at −80 °C for subsequent analysis.

Immunofluorescence analysis

Frozen slices were removed from the refrigerator and placed at room temperature for more than 30 min. The sections were boiled in 0.01 M citric acid buffer for 10 min for antigen retrieval. Next, the sections were soaked in 1% Triton-100 for 10 min to increase the cell membrane permeability to antibodies. The frozen sections were soaked in 0.1 M PBS three times for 5 min each time. They were then blocked with 5% bovine serum albumin (BSA) at room temperature for 30 min to eliminate nonspecific binding. After that, the frozen sections were incubated with primary antibodies that included anti-tyrosine hydroxylase (TH) (1:200, Santa Cruz Biotechnology, Dallas, TX, USA), anti-glial fibrillary acidic protein (GFAP) (1:500, Dako, Denmark), anti-ionized calcium binding adapter molecule-1 (IBA-1) (1:500, Wako, Japan), anti-CD16/32 (1:100, BD Biosciences Pharmingen, San Jose, CA, USA), anti-CD206 (1:200, R&D Systems, Minneapolis, MN, USA), and anti-NF-κB p65 (1:200, Santa Cruz Biotechnology), overnight at 4 °C. After washing with PBS solution containing 0.2% Tween-20 (PBST) three times, the sections were incubated with Alexa Fluor 488-conjugated donkey anti-rabbit IgG (Invitrogen, Carlsbad, CA, USA) or Alexa Fluor 488-conjugated donkey anti-mouse IgG (Invitrogen) or Alexa Fluor 488-conjugated donkey anti-goat IgG (Invitrogen), Alexa Fluor 546-conjugated donkey anti-mouse IgG (Invitrogen) and Hoechst 33342 (Beyotime Biotechnology, Shanghai, China) in PBS containing 3% BSA for 2 h at room temperature and away from light. After washing with PBST for 5 min 3 times in the dark, the sections were mounted with 90% (*v*/*v*) glycerol and sealed with nail oil. Finally, images were captured with a confocal laser scanning microscope (TCS SP2, Leica, Solms, Germany) in the dark, and the fluorescence intensity was analyzed by Image-Pro Plus 6.0 software (Media Cybernetics, Silver Springs, MD, USA).

Quantitative PCR (qPCR)

Frozen midbrain tissue was removed from the −80 °C refrigerator and weighed. Tissues were placed in a tube with TRIzol Reagent (Invitrogen, Carlsbad, CA, USA) and lysis buffer and homogenized with a cold homogenizer. Total RNA was separated and extracted by chloroform, isopropanol, and other reagents. The concentration and purity of RNA were measured by a nanometer ultra-micro nucleic acid analyzer. Reverse transcription of 1 μg total RNA into cDNA was performed using the TransScript One-Step gDNA Removal and cDNA Synthesis kit (TransGen Biotech, Beijing, China). The TransStart Tip Green qPCR Supermix kit (TransGen

Table 1. Primers for qPCR analysis

Gene	Forward primer	Reverse primer
TNF-α	5′-AGGCACTCCCCCAAAAGATG-3′	5′-TGAGGGTCTGGGCCATAGAA-3′
IL-1β	5′-GTGGCAGCTACCTGTGTCTT-3′	5′-GGAGCCTGTAGTGCAGTTGT-3′
IL-6	5′-TCCAGTTGCCTTCTTGGGAC-3′	5′-GACAGGTCTGTTGGGAGTGG-3′
IL-10	5′-CACCTACTTCCCAGCCAACC-3′	5′-TCAGCAGAGACTCACTCAGCAAC-3′
M1		
iNOS	5′-CAAGCACCTTGGAAGAGGAG-3′	5′-AAGGCCAAACACAGCATACC-3′
CD16	5′-TTTGGACACCCAGATGTTTCAG-3′	5′-GTCTTCCTTGAGCACCTGGATC-3′
CD32	5′-AATCCTGCCGTTCCTACTGATC-3′	5′-GTGTCACCGTGTCTTCCTTGAG-3′
M2		
Arg1	5′-TCACCTGAGCTTTGATGTCG-3′	5′-CTGAAAGGAGCCCTGTCTTG-3′
CCL-22	5′-CTGATGCAGGTCCCTATGGT-3′	5′-GCAGGATTTTGAGGTCCAGA-3′
TGF-β	5′-TGCGCTTGCAGAGATTAAAA-3′	5′-CGTCAAAAGACAGCCACTCA-3′
Internal control		
GAPDH	5′-TCATTGACCTCAACTACATGGT-3′	5′-CTAAGCAGTTGGTGGTGCA-3′

Biotech) and Line Gene 9600 Plus fluorescence quantitative PCR detection system (Bioer Technology, Hangzhou, China) were used to amplify the cDNA. Relative quantitative analysis was used to analyze the amplification results. The primer sequences are shown in Table 1.

Western blotting analysis

Brain tissue was weighed in a test tube. Ten-fold (*w/v*) ice-cold RIPA buffer (Beyotime, Shanghai, China) with protease inhibitor cocktail (Thermo Fischer Scientific, Waltham, MA, USA) and phosphatase inhibitors (Thermo Fischer Scientific, Waltham, MA, USA) was added to the test tube, and the tissue was homogenized with a cold homogenizer. Then, the test tube was placed in the ice-water bath for 30 min, accompanied by shaking. After centrifugation, the supernatants were retrieved. The protein concentrations were measured with a BCA kit (Applygen, Beijing, China). The remaining protein supernatants were mixed with 5× loading buffer at a ratio of 1:4 and then boiled for 15 min to denature the protein. Then, 30 μg of denatured protein per sample was separated on 12% (*w/v*) SDS-PAGE gels and transferred to PVDF membranes (Millipore, Bedford, MA, USA). The PVDF membranes were blocked with 5% (*w/v*) BSA (Sigma-Aldrich, St. Louis, MO, USA) at room temperature for 2 h and then incubated with one of the following primary antibodies at 4 °C overnight: anti-TH (1:500, Santa Cruz Biotechnology, Santa Cruz, CA, USA), anti-IBA-1 (1:500, Abcam, Cambridge, UK), anti-GFAP (1:500, Abcam), anti-TNF-α (1:200, Santa Cruz Biotechnology), anti-IL-1β (1:200, Santa Cruz Biotechnology), anti-IL-6 (1:200, Santa Cruz Biotechnology), anti-IL-10 (1:200, Santa Cruz Biotechnology), anti-TGF-β (1:500, Abcam), anti-BDNF (1:1000, Cell Signaling Technology, Beverly, MA, USA), and anti-beta-actin (1:5000, Sigma-Aldrich, St. Louis, MO, USA). After washing with TBST buffer three times for 10 min, the PVDF membranes were incubated with the appropriate AffiniPure-conjugated corresponding secondary antibodies (1:5000, KPL, Gaithersburg, MD, USA) at room temperature for 2 h with mild shaking. After thorough washing with TBST buffer three times for 10 min, the protein bands were detected with an enhanced chemiluminescence plus detection system (GE, Fairfield, CT, USA). Analysis of the immunoreactivity of each protein was performed using image analysis software (NIH, Bethesda, MD, USA).

The three midbrain tissues in each group were processed with a cytoplasm/nucleus separation kit, and the total proteins in the cytoplasm and nucleus were obtained. After the protein supernatants were quantified by a BCA kit, Western blotting was performed. The PVDF membranes were incubated with anti-NF-κB p65 (1:1000, Santa Cruz, Santa Cruz, CA, USA), anti-PCNA (1:200, Santa Cruz, Santa Cruz, CA, USA), and anti-beta-actin (1:5000, Sigma-Aldrich, St. Louis, MO, USA). The other steps were as mentioned above.

Statistical analysis

All experimental data are expressed as the mean ± SD and were analyzed by SPSS21.0 software (SPSS Inc., Chicago, IL, USA). The data were derived from at least three independent experiments. One-way analysis of variance (ANOVA) followed by Duncan's multiple range test (DMRT) was used in the analysis method. $P < 0.05$ was considered to indicate statistical significance.

RESULTS

Rg1 ameliorates the behavioral disorders and mortality induced by LPS

Mice were treated with LPS and Rg1 to assess the effect of Rg1 on behavioral disorders. As shown in Fig. 2a, mice showed significant behavioral impairment in the rotating rod test ($P < 0.001$), as manifested by decreased latency to fall from the rotating rod in the model group compared to the vehicle group. Pretreatment with Rg1 at doses of 20 mg/kg ($P < 0.001$) and 40 mg/kg ($P < 0.001$) significantly attenuated this effect. Similarly, the mice that received the positive drug also significantly improved the behavioral disorders ($P < 0.001$). There was no significant difference between the control and vehicle groups ($P > 0.05$).

In the pole test (Fig. 2b), the model group mice spent more time climbing from the top to the bottom of the wooden pole ($P < 0.001$), suggesting bradykinesia. Of note, the Rg1 20 mg/kg ($P < 0.01$) and 40 mg/kg ($P < 0.001$) groups exhibited improved behavior in the pole test. The positive control drug could also improve this behavioral disorder ($P < 0.01$). The control group and vehicle group were not significantly different ($P > 0.05$).

There was a statistically significant difference in the basic grip between the vehicle group and the model group ($P < 0.01$). As shown in Fig. 2c, 40 mg/kg Rg1 could improve the reduction in the mouse basic grip ($P < 0.05$). Grip strength in the control mice had no significant correlation with the grip strength of the vehicle mice ($P > 0.05$). These results suggested that Rg1 treatment significantly attenuated the behavioral dysfunction induced by LPS.

A common problem with this subacute PD model is the death of mice during LPS injection for five days. None of the control

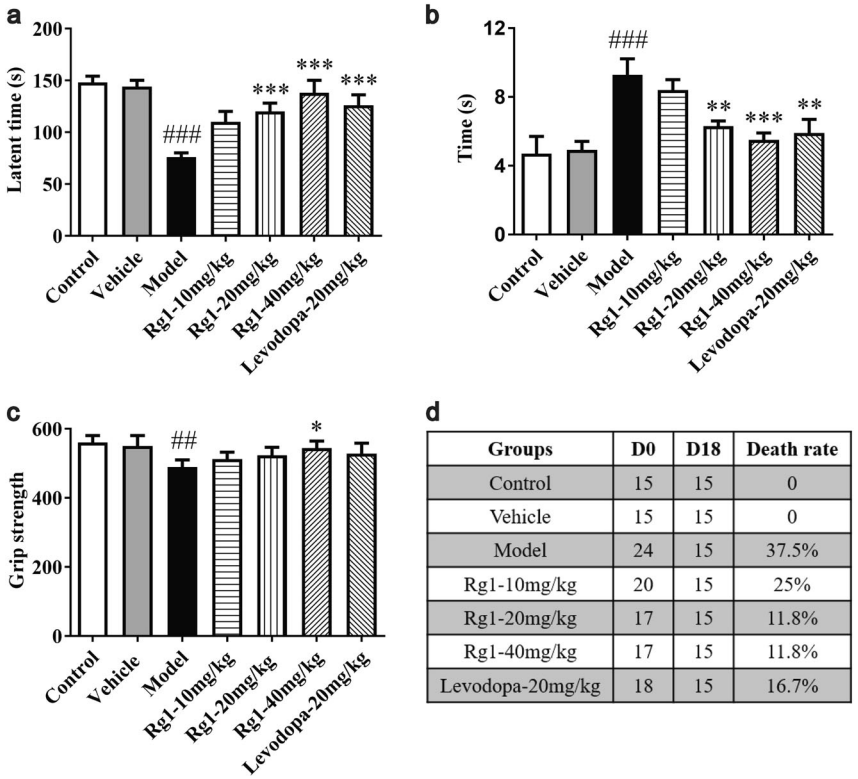

Groups	D0	D18	Death rate
Control	15	15	0
Vehicle	15	15	0
Model	24	15	37.5%
Rg1-10mg/kg	20	15	25%
Rg1-20mg/kg	17	15	11.8%
Rg1-40mg/kg	17	15	11.8%
Levodopa-20mg/kg	18	15	16.7%

Fig. 2 Neuroprotective effect of Rg1 against the LPS-induced death rate and behavior defects. **a** Protective effect of Rg1 on motor coordination in the rotarod test. **b** Protective effect of Rg1 on bradykinesia in the pole test. **c** Protective effect of Rg1 in the grip strength test. **d** Animal death rate across experimental groups. $^{\#\#}P < 0.01$, $^{\#\#\#}P < 0.001$ vs. vehicle group; $^{*}P < 0.05$, $^{**}P < 0.01$, $^{***}P < 0.001$ vs. model group. All data were presented as mean ± SD of triplicate independent experiments

mice died by D18, whereas the death rate was 37.5% in the model group, indicating that LPS has a certain lethal effect on mice (Fig. 2d). Rg1 treatment prior to LPS administration resulted in reduced death rates in the Rg1 10 mg/kg group (25%), the Rg1 20 mg/kg group (11.8%) and the Rg1 40 mg/kg group (11.8%). Levodopa reduced the death rate to 16.7%.

Rg1 improves the loss of dopaminergic neurons in the SN induced by LPS

To investigate the effect of Rg1 on the neurotoxicity in the SN induced by LPS, we observed the number of TH-positive dopamine neurons in the SN. As shown in Fig. 3a, c, we found that TH protein and TH-positive dopamine neuron levels were lower in the SN of LPS-treated mice in comparison to the vehicle group ($P < 0.001$), which further confirmed that the PD model was successfully established in mice. Remarkably, Rg1 administration dramatically reversed the decreased expression of TH protein induced by LPS ($P < 0.001$). Consistent with the above findings, the immunofluorescent analysis of the SN further demonstrated that 20 mg/kg Rg1 ($P < 0.01$) and 40 mg/kg Rg1 ($P < 0.001$) could significantly improve the reduction of TH-positive immune cells induced by LPS. Similarly, Western blot and immunofluorescent analysis indicated that TH-positive cells ($P < 0.01$) and TH protein ($P < 0.001$) expression levels were significantly increased by levodopa compared to those in the model group.

Rg1 suppresses the activation of glial cells in the SNpc induced by LPS

Neuroinflammation, characterized by overactivation of glial cells, plays an important role in the degeneration and death of DA neurons in the SNpc of PD [22]. As shown in Fig. 4a, d, LPS exposure caused severe gliosis in the SNpc. IBA-1 is a well-known marker of microglia [23]. The number of IBA-1 and GFAP immunoreactive cells was significantly increased by LPS compared to that in the vehicle group ($P < 0.001$). Rg1 attenuated the response of IBA-1-positive microglia and GFAP-positive astrocytes induced by LPS treatment in a dose-dependent manner, especially in the high-dose groups ($P < 0.01$). Similar findings were observed for IBA-1 and GFAP protein expression levels: Rg1 showed inhibitory effects on LPS-induced glial activity, as evidenced by reduced IBA-1 ($P < 0.001$) and GFAP levels ($P < 0.05$). Furthermore, Western blot and immunofluorescent assays suggested that the LPS-induced increase in IBA-1 and GFAP levels was reversed in levodopa-treated groups. Together, the findings illustrated that Rg1 attenuated astrocyte and microglial activation and protected neurons from LPS-induced damage.

Rg1 alleviates the inflammatory response induced by LPS

LPS can induce proinflammatory cytokine release, leading to neuroinflammation [24]. TNF-α, IL-1β, IL-6, and IL-10, etc. levels in the substantia nigra tissue were explored here to calculate the effects of Rg1 on LPS-induced neuroinflammation. The results indicated that LPS treatment induced a higher level of TNF-α, IL-1β, and IL-6 expressions compared to the vehicle treatment ($P < 0.001$), and Rg1 administration downregulated these inflammatory markers in the SN of mice induced by LPS, as demonstrated by qPCR methods (Fig. 5a). TNF-α mRNA detection results indicated that levodopa group also had markedly decreased proinflammatory cytokine expression compared to the model group ($P < 0.001$). In contrast, 20 mg/kg Rg1 ($P < 0.01$), 40 mg/kg Rg1 ($P < 0.001$), and levodopa ($P < 0.01$) significantly increased the mRNA level of IL-10 after LPS insult.

Moreover, the protein levels of TNF-α, IL-1β, and IL-6 decreased markedly with Rg1 treatment. As shown in Fig. 5b, protein detection and histogram results showed that Rg1 could shift harmful inflammation toward a more favorable direction,

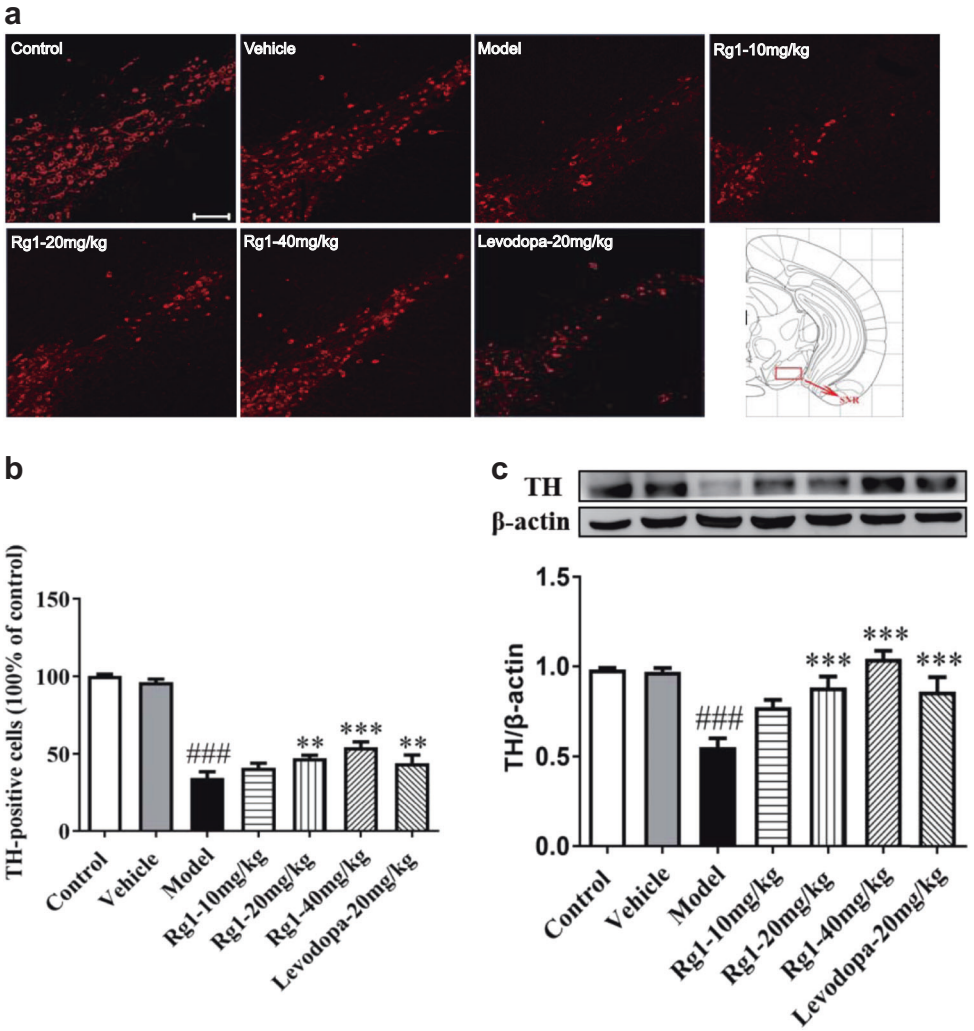

Fig. 3 Rg1 restored the reduction of TH-positive neurons and protein expression in the substantia nigra pars compacta (SNpc) induced by LPS. **a** Representative immunofluorescence images of TH-immunoreactive neurons across groups (scale bar = 100 μm). **b** A histogram representing the quantitative analysis of TH-positive cells normalized to control levels is shown. Representative protein bands of TH and b-actin and histogram representing the quantitative analysis of TH levels normalized to β-actin protein levels are shown. **c** Representative protein bands of TH and β-actin and the histograms representing the quantitative analysis of TH levels normalized to β-actin protein levels are shown. All data are presented as mean ± SD of triplicate independent experiments. $^{###}P < 0.001$ vs. vehicle group; $^{**}P < 0.01$, $^{***}P < 0.001$ vs. model group. All data are presented as mean ± SD of triplicate independent experiments

significantly increasing the protein expression of anti-inflammatory cytokines and neurotrophin. Similar findings were observed after levodopa treatment: proinflammatory cytokine protein levels were significantly reduced. The anti-inflammatory cytokines TGF-β and IL-10 and the neurotrophic factor BDNF, which are beneficial for neuronal survival and brain repair, all increased markedly (Fig. 5b). Together, the findings illustrated that Rg1 exerted neuroprotective effects by suppressing the inflammatory response.

Rg1 regulates the polarization balance of microglia in the SN induced by LPS

Based on the research above, Rg1 was suggested to contribute to preventing LPS-induced neuroinflammation in mice. To further confirm its neuroprotective role in PD, the expression levels of polarization markers of microglia were observed using immunofluorescent and real-time PCR (qPCR) analysis. Since M1 and M2 phenotypes, respectively, represent pro-inflammatory and anti-inflammatory activity of microglia in response to neuroinflammation, we analyzed the effects of Rg1 on the mRNA expression of M1 markers (iNOS, CD16, and CD32) and M2 markers (Arg1, CCL22, and TGF-β) [25, 26]. As shown in Fig. 6a, LPS significantly increased the mRNA expression of M1 polarization markers ($P < 0.001$). Next, CD16/32 and CD206 were costained with IBA-1 for relevant histological cell levels analysis [27]. As shown in Fig. 6b, the immunofluorescence intensity of CD16/32 increased significantly after LPS attack, while that of CD206 showed a small but not insignificant increase. The detection of these polarized markers indicated that Rg1 inhibited the M1 phenotypic polarization of microglia and skewed it toward M2 phenotype polarization in a dose-dependent manner. Our results indicated that Rg1 improved PD-like symptoms in mice by regulating the polarization balance of microglia.

Rg1 inhibits nuclear translocation of NF-κB induced by LPS

Since the NF-κB pathway is a key factor in regulating the M1/M2 balance in microglia cells [28], we investigated whether it could exert its polarization balance regulatory effects by inhibiting NF-κB nuclear translocation. Using Western blot analysis and immunofluorescence, we demonstrated that the expression of NF-κB in the nucleus in the model group was significantly higher than that in

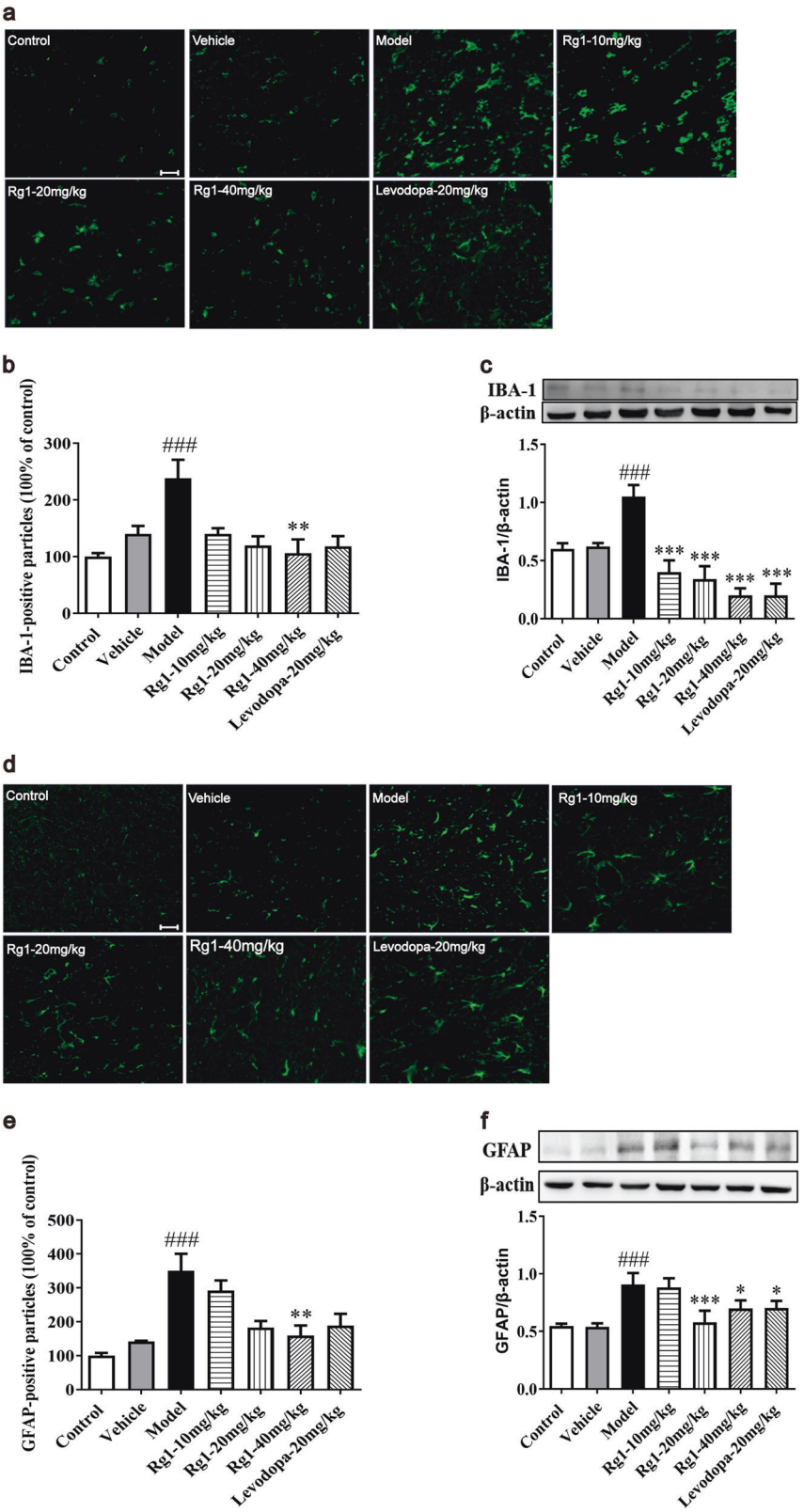

Fig. 4 Rg1 attenuates glial activation induced by LPS in the SNpc. **a**, **d** Representative immunofluorescence images of IBA-1 and GFAP immunoreactive cells in the SNpc (scale bar = 20 μm). **b**, **e** Two histograms representing the respective quantitative analysis of IBA-1-positive and GFAP-positive cells normalized to control levels are shown. **c**, **f** Representative protein bands of IBA-1, GFAP, and β-actin and the histograms representing the quantitative analysis of IBA-1 or GFAP levels normalized to β-actin protein levels are shown. All data were presented as mean ± SD of triplicate independent experiments. $^{###}P < 0.001$ vs. vehicle group; $^{*}P < 0.05$, $^{**}P < 0.01$, $^{***}P < 0.001$ vs. model group

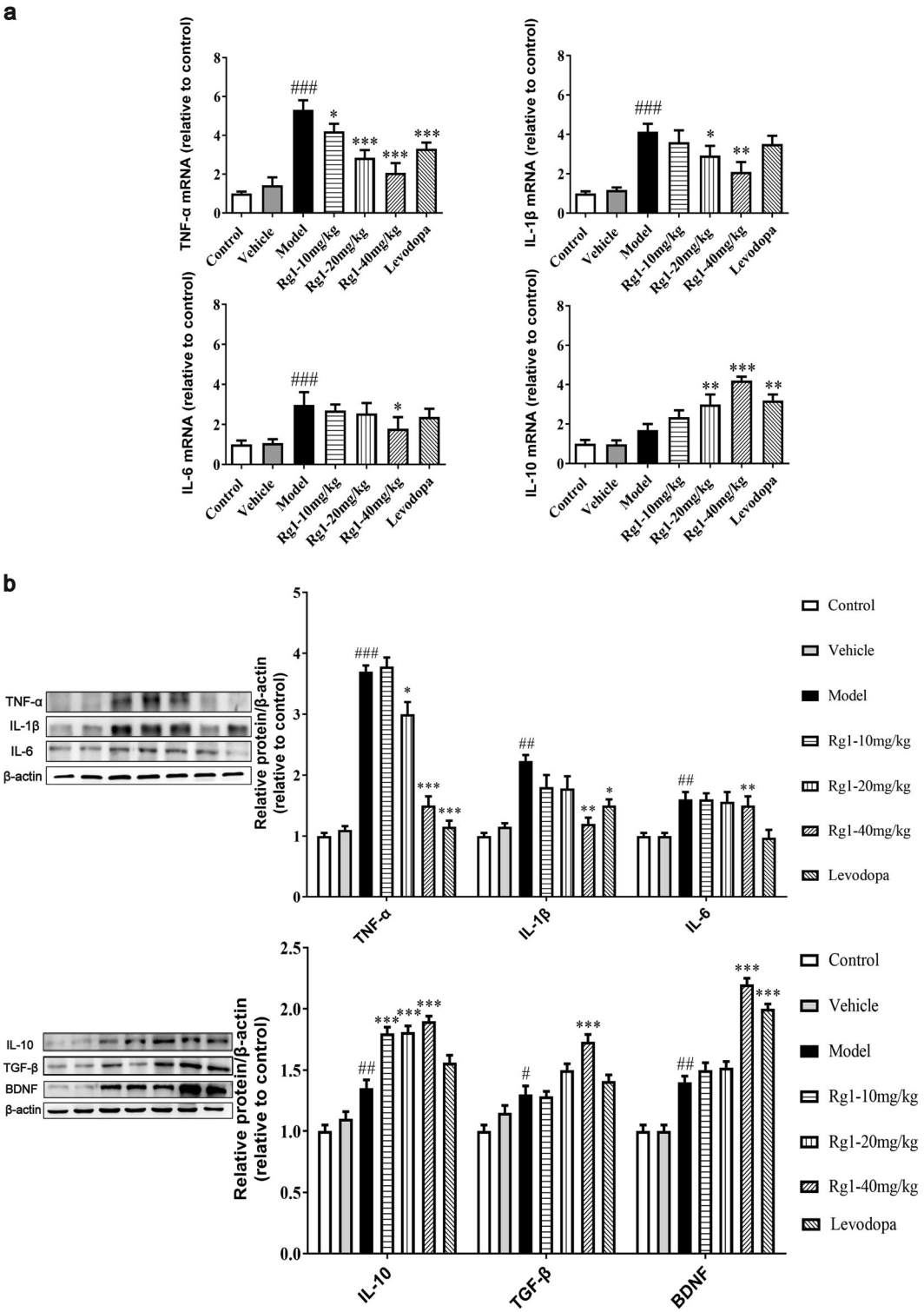

Fig. 5 Rg1 alleviates the inflammatory response in LPS-injured PD mice. **a** Expression of TNF-α, IL-1β, IL-6, and IL-10 in the mice midbrain were determined using qPCR. **b** Representative blots and densitometry data for TNF-α, IL-1β, IL-6, IL-10, BDNF, and TGF-β. All data were presented as mean ± SD of triplicate independent experiments. $^{\#}P < 0.05$, $^{\#\#}P < 0.01$, $^{\#\#\#}P < 0.001$ vs. vehicle group; $^{*}P < 0.05$, $^{**}P < 0.01$, $^{***}P < 0.001$ vs. model group

the vehicle group (Fig. 7a, b). The expression of NF-κB in the nucleus was significantly reduced by Rg1 treatment. These data indicated that in the LPS-lesioned SN of mice, Rg1 inhibited LPS-induced NF-κB accumulation in the nucleus to participate in the regulation of microglia polarization balance, which was consistent with the previous hypothesis.

DISCUSSION

In these studies, it was found that Rg1 significantly reduced mouse mortality, motor deficits and loss of dopamine neurons in the SN. Mechanistic studies showed that the anti-neuroinflammatory properties of Rg1 may be involved in the neuroprotective effect. Rg1 treatment obviously inhibited the activation of microglia and

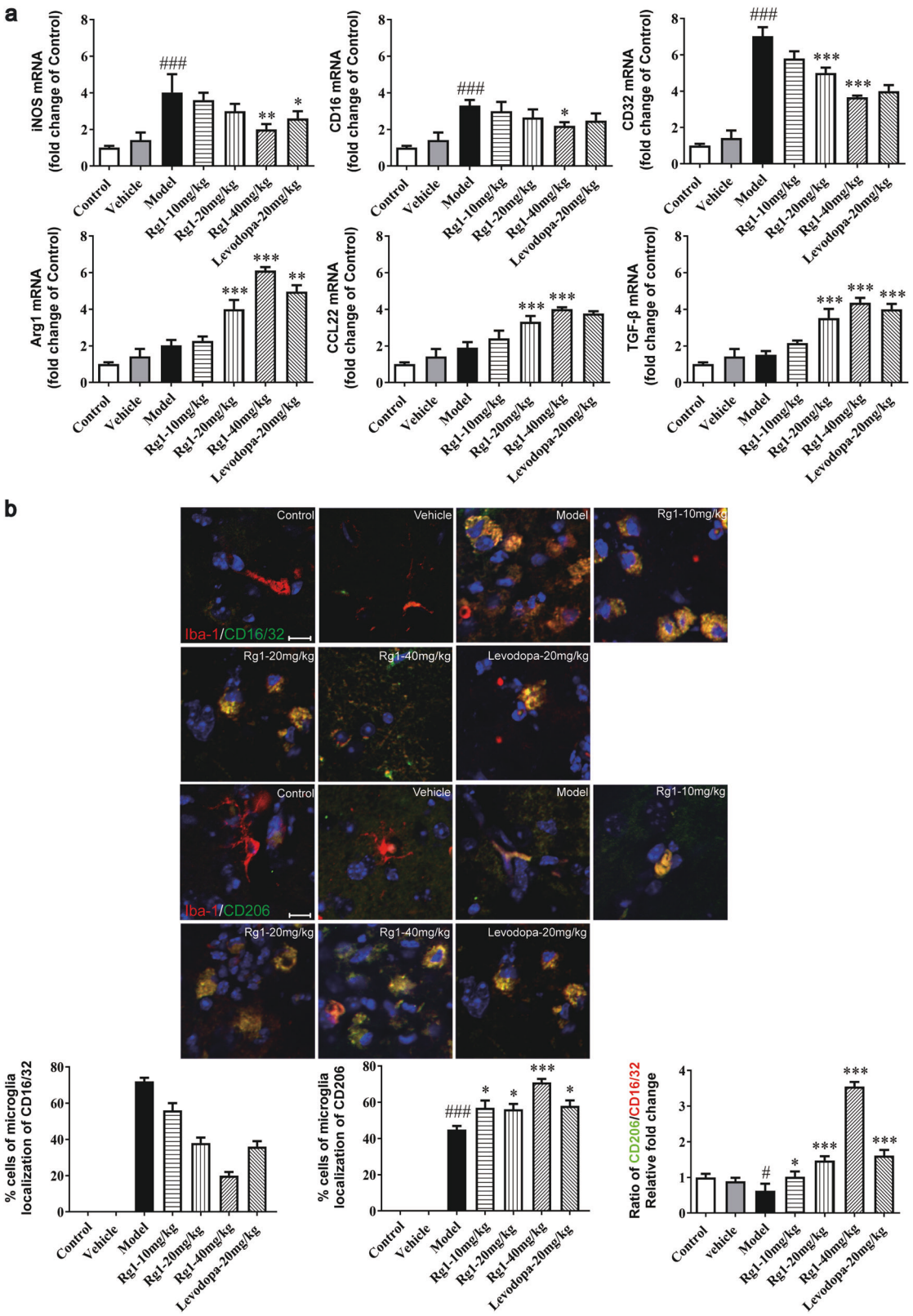

Fig. 6 Rg1 regulated the M1 and M2 activation states. **a** qPCR analysis of mRNA expression of M1 markers (iNOS, CD16, CD32) and M2 markers (Arg1, CCL-22, TGF-β) in the midbrain of LPS-PD mice. **b** Representative photomicrographs of double-staining immunofuorescence of CD16/32 with Iba-1 and CD206 with Iba-1 in the midbrain of LPS-induced PD mice. Quantitative analysis of CD16/32-positive and CD206-positive microglia in the midbrain (scale bar = 10 μm). All data were presented as mean ± SD of triplicate independent experiments. $^{\#}P < 0.05$, $^{\#\#\#}P < 0.001$ vs. vehicle group; $^{*}P < 0.05$, $^{**}P < 0.01$, $^{***}P < 0.001$ vs. model group

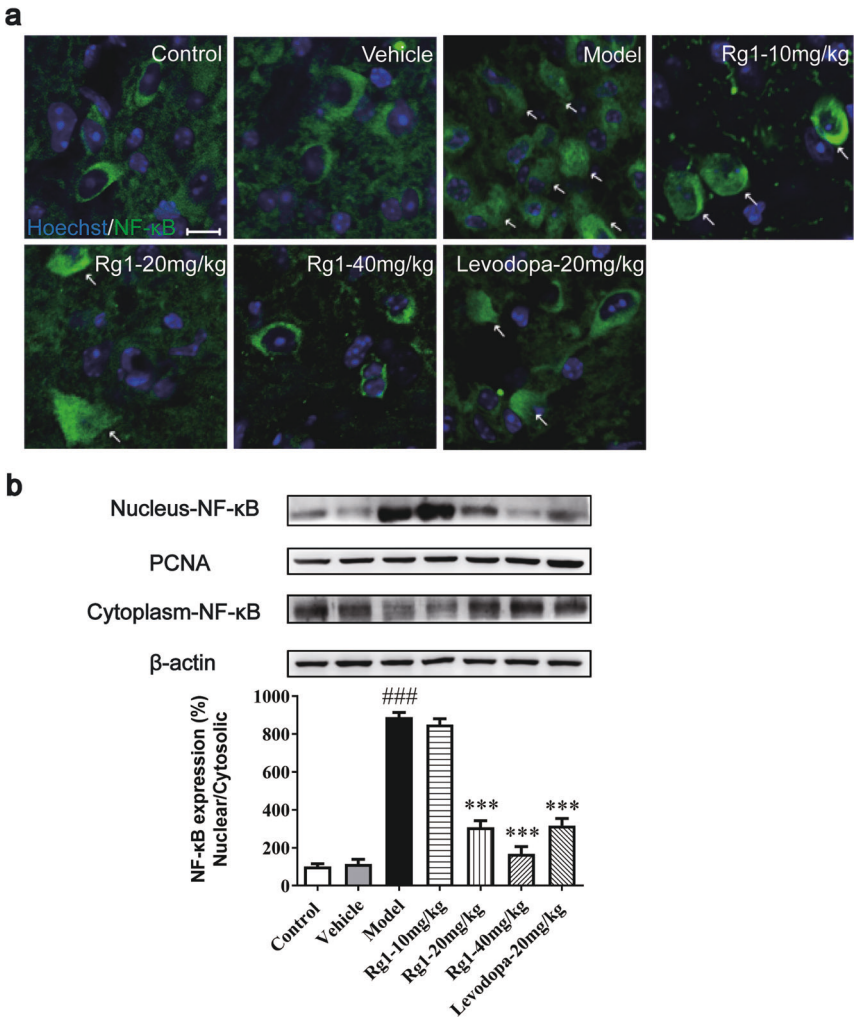

Fig. 7 Effect of Rg1 on the transcriptional activity of NF-κB. **a** Translocation of NF-κB toward the nucleus determined by Immunofluorescence staining (scale bars = 10 μm). **b** Representative blots and densitometry data for nucleus/cytoplasm NF-κB ratio in the midbrain microglia. All data were presented as mean ± SD of triplicate independent experiments. $^{###}P < 0.001$ vs. vehicle group; $^{***}P < 0.001$ vs. model group

astrocytes in the SN. Proinflammatory cytokines such as TNF-α, IL-1β, and IL-6 were remarkably reduced, while anti-inflammatory cytokines and neurotrophin were increased significantly. Finally, we determined that Rg1 significantly reduced the M1 phenotype of microglia, skewing them toward the M2 phenotype, by inhibiting NF-κB nuclear translocation. Rg1 may modulate neuroinflammation by regulating microglia polarization dynamics and nuclear translocation of NF-κB.

In this investigation, we established a subacute PD mouse model by injecting LPS into the SN for 5 consecutive days. LPS, as an inflammatory inducer, cannot destroy the permeability of the blood–brain barrier (BBB) by peripheral injection [6]. Moreover, since dopaminergic neurons and microglia are located in common areas and dopaminergic neurons are more susceptible to inflammation-mediated damage, this model is more likely to cause selective damage of dopaminergic neurons [29]. Therefore, this model is more suitable to mimic the etiology of inflammation-mediated PD.

In this PD model, considering the multiple stereotaxic injections of LPS in the SN, it is easy to increase the mortality due to mechanical/surgical injury. Hence, we introduced a dual-guide cannula micro dosing system to optimize and improve the traditional rat model of LPS injection in the SN, greatly reducing the mortality caused by multiple stereotaxic injections in the SN and the site error of each injection [20, 30].

Intracerebral inflammation can cause death in PD patients [31, 32]. The mortality of LPS-induced PD mice was not reported in previous studies, but we demonstrated for the first time that 10, 20, and 40 mg/kg Rg1 treatment decreased mouse mortality by 12.5%, 25.7%, and 25.7%, respectively, compared to that in the LPS-only group. LPS could induce the majority of parkinsonian symptoms, including body stiffness, unstable posture, and some signs of tremor, which were consistent with the clinical motor symptoms of PD patients. Here, the rotarod test was used to observe the motor balance regulation ability, the pole test was used as an indicator of muscle coordination, and the grip strength test was used to test the influence of nerve injury on muscle strength [33–35]. Based on these results, Rg1 indeed improved LPS-induced PD-like symptoms in mice. To exclude the interference by pre-implanted tubes on the behavioral results of mice, the animals were rested for 8 days after the implantation, and pre-implanted mice were randomly divided into groups.

Recent studies have shown that neuroinflammation accompanies the occurrence and progression of PD. Neurotoxicity mediated by neuroinflammation plays an important role in the cascade of neuronal death in PD. The activation of immune glial cells including microglia and astrocytes in the central nervous system (CNS) is a major feature of neuroinflammation. Astrocytes are considered the primary target of the offending agent, and they

exhibited rounded cell bodies and shrunken neurites that tended to be close together after activation. Activated microglia showed enlarged cell bodies and an amoeba-like appearance, and the number of neurites decreased. Microglia may rapidly migrate to the lesion by morphological changes after activation. As early as 1998, Mcgeer found a large number of reactive microglia in the SN of PD patients [36]. Previous research has also confirmed that abnormally activated microglia could cause toxic effects on dopaminergic neurons by secreting a large number of inflammatory cytokines, such as TNF-α and IL-1β, thereby causing damage, which is in line with our data. Furthermore, our data showed that Rg1 could protect DA neurons by reducing proinflammatory cytokines and increasing the secretion of anti-inflammatory cytokines (TGF-β and IL-10) and neurotrophin (BDNF). However, the specific mechanisms of the neuroprotective effect of Rg1 on PD mice need to be further investigated.

The above discussion has demonstrated that microglia play a pivotal role in LPS-induced subacute PD mice. It has long been demonstrated that activated microglia may polarize similarly to peripheral macrophages in the CNS toward the proinflammatory M1 phenotype or the anti-inflammatory M2 phenotype through the production of cytokines [37]. Studies have shown that M1-polarized microglia decrease cell survival, proliferation, differentiation and other functions by releasing pro-inflammatory mediators and cytotoxic substances, resulting in nonspecific damage to neuronal function. The M2 polarized microglia could accelerate the removal of necrotic tissues and the repair of normal tissues through enhancement of their phagocytic function. Thus, modulating microglial polarization may be a potential target for PD therapy. Therefore, we focused on microglia polarization in this study. It seems noteworthy that the expression of M1 markers (iNOS, CD16, and CD32) increased significantly in this work, indicating that the microglia polarized to the M1 phenotype in the LPS-lesioned SN. Furthermore, it has been reported that Rg1 attenuates the M1-type polarization and tends to favor the M2 polarization phenotype [38]. This is in line with our data showing that the expression of M2 phenotypic markers (Arg1, CCL-22, TGF-β, and CD206) increased in the Rg1 groups [39]. Based on the above investigations, we believe that Rg1 plays a neuroprotective role in LPS-induced subacute PD mice by regulating the polarization of microglia.

NF-κB is regarded as a central transcription factor of inflammatory mediators, which play an important role in the activation of microglia [28]. A great deal of research has shown that the development of PD is accompanied by the activation of NF-κB, which is a key factor in regulating the M1/M2 paradigm. In this study, we found that LPS insult caused NF-κB activation in the SN of subacute PD mice, which could be attenuated by Rg1 administration. This suggests that Rg1 may drive microglia to the M2 phenotype through the NF-κB pathway.

In conclusion, our findings demonstrate that Rg1 exhibits a neuroprotective effect in the subacute LPS-induced parkinsonism mouse model. Rg1 prevented the neurodegeneration induced by LPS by attenuating glial activation, proinflammatory cytokine release and increasing anti-inflammatory cytokine and neurotrophin release. In addition, the anti-neuroinflammatory effects of Rg1 were closely related to its ability to regulate microglia polarization dynamics, accompanied by nuclear translocation of NF-κB (Fig. 8). These findings will provide new candidate targets

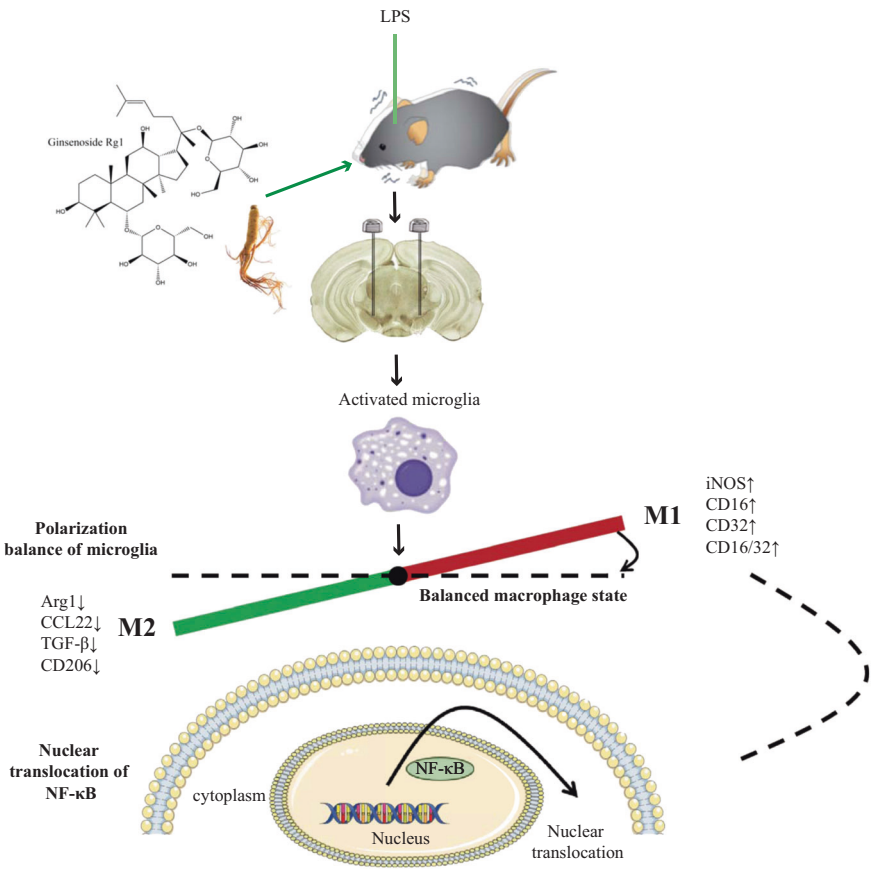

Fig. 8 Schematic diagram of the neuroprotective effect of Rg1 in LPS-induced subacute PD mice by microglial polarization regulation. Continuous injection of LPS into the SN of mice resulted in polarization of activated microglia cells in the midbrain to pro-inflammatory M1 phenotype, accompanied by increased expression of markers (iNOS, CD16, CD32, and CD16/32). Rg1 modulates microglia toward a lower M1 phenotype polarization and higher M2 phenotype polarization in the SN of PD mice, which was accompanied by reducing the nuclear translocation of NF-κB, leading to increased expression of markers (Arg1, CCL22, TGF-β, and CD206) and improvement of PD-like symptoms

and ideas for the development of drugs to treat PD, as well as provide data for Rg1 preclinical research.

ACKNOWLEDGEMENTS

This work was supported by the National Natural Science Foundation of China Grants (81503275, 81973499, 81603316, 81873026, 81730096, 81172934, and 30973607), the CAMS Innovation Fund for Medical Sciences (CIFMS) (2016-I2M-1-004) and "Double First-Class" New Drug Development Project of China Pharmaceutical University (CPU2018PZQ15).

AUTHOR CONTRIBUTIONS

JQL, MZ, and SFC conceived and designed the experiments; JQL performed most of the experiments and analyzed the data, as well as drafted and revised the paper; LYC and XZ helped to prepare the animal models; ZZ and SFC revised the paper; DYZ and NHC were involved in the interpretation of the data.

ADDITIONAL INFORMATION

Competing interests: The authors declare no competing interests.

REFERENCES

1. Stochl J, Boomsma A, Ruzicka E, Brozova H, Blahus P. On the structure of motor symptoms of Parkinson's disease. Mov Disord. 2010;23:1307–12.
2. Kim YS, Joh TH. Microglia, major player in the brain inflammation: their roles in the pathogenesis of Parkinson's disease. Exp Mol Med. 2006;38:333–47.
3. Iarlori C. Anti-inflammatory agents in Parkinson's disease. Former Curr Medicinal. 2009;8:72–84.
4. Lu L. Novel anti-inflammatory and neuroprotective agents for parkinsons disease. CNS Neurol Disord Drug Targets. 2010;9:232–40.
5. Li DW, Zhou FZ, Sun XC, Li SC, Yang JB, Sun HH, et al. Ginsenoside Rb1 protects dopaminergic neurons from inflammatory injury induced by intranigral lipopolysaccharide injection. Neural Regen Res. 2019;14:1814–22.
6. Bickel U, Grave B, Kang YS, del RA, Voigt K. No increase in blood-brain barrier permeability after intraperitoneal injection of endotoxin in the rat. J Neuroimmunol. 1998;85:131–6.
7. He Q, Yu W, Wu J, Chen C, Lou Z, Zhang Q, et al. Intranasal LPS-mediated Parkinson's model challenges the pathogenesis of nasal cavity and environmental toxins. PLoS ONE. 2013;8:e78418.
8. Pisanu A, Lecca D, Mulas G, Wardas J, Simbula G, Spiga S, et al. Dynamic changes in pro- and anti-inflammatory cytokines in microglia after PPAR-γ agonist neuroprotective treatment in the MPTPp mouse model of progressive Parkinson's disease. Neurobiol Dis. 2014;71:280–91.
9. Bok E, Chung YC, Kim KS, Baik HH, Shin WH, Jin BK. Modulation of M1/M2 polarization by capsaicin contributes to the survival of dopaminergic neurons in the lipopolysaccharide-lesioned substantia nigra in vivo. Exp Mol Med. 2018;50:76.
10. Mao Y, Wang B, Xu X, Du W, Li W, Wang Y. Glycyrrhizic acid promotes M1 macrophage polarization in murine bone marrow-derived macrophages associated with the activation of JNK and NF-κB. Mediators Inflamm. 2015;2015:372931.
11. Mogi M, Kondo T, Mizuno Y, Nagatsu T. p53 protein, interferon-gamma, and NF-kappaB levels are elevated in the parkinsonian brain. Neurosci Lett 2007;414:94–7.
12. Daily D, Vlamis-Gardikas A, Offen D, Mittelman L, Melamed E, Holmgren A, et al. Glutaredoxin protects cerebellar granule neurons from dopamine-induced apoptosis by dual activation of the ras-phosphoinositide 3-kinase and jun n-terminal kinase pathways. J Biol Chem 2001;276:21618–26.
13. Lee YJ, Chung E, Lee KY, Lee YH, Huh B, Lee SK. Ginsenoside-Rg1, one of the major active molecules from Panax ginseng, is a functional ligand of glucocorticoid receptor. Mol Cell Endocrinol 1997;133:135–40.
14. Ren XF, Chen L, Gao XQ, Xie JX, Chen WF. Glucocorticoid receptor is involved in the neuroprotective effect of ginsenoside Rg1 against inflammation-induced dopaminergic neuronal degeneration in substantia nigra. J Steroid Biochem Mol Biol 2016;155(Pt A):94–103.
15. Zhang Y, Hu W, Zhang B, Yin Y, Zhang J, Huang D, et al. Ginsenoside Rg1 protects against neuronal degeneration induced by chronic dexamethasone treatment by inhibiting NLRP-1 inflammasomes in mice. Int J Mol Med 2017;40:1134.
16. Reale M, Iarlori C, Thomas A, Gambi D, Perfetti B, Onofrj M, et al. Peripheral cytokines profile in Parkinson's disease. Brain Behav Immun 2009;23:55–63.
17. Heng Y, Zhang QS, Mu Z, Hu JF, Yuan YH, Chen NH. Ginsenoside Rg1 attenuates motor impairment and neuroinflammation in the MPTP-probenecid-induced parkinsonism mouse model by targeting α-synuclein abnormalities in the substantia nigra. Toxicol Lett 2016;243:7–21.
18. Chen Y, Chen XC. [Possible mechanisms of the protective effect of ginsenoside Rg1 on apoptosis in substantia nigra neurons]. Yao Xue Xue Bao 2002;37:249–52.
19. Chen XC, Zhou YC, Chen Y, Zhu YG, Fang F, Chen LM. Ginsenoside Rg1 reduces MPTP-induced substantia nigra neuron loss by suppressing oxidative stress. Acta Pharm Sin 2005;26:56–62.
20. Tanaka S, Ishii A, Ohtaki H, Shioda S, Yoshida T, Numazawa S. Activation of microglia induces symptoms of Parkinson's disease in wild-type, but not in IL-1 knockout mice. J Neuroinflammation 2013;10:143.
21. Ogawa N, Hirose Y, Ohara S, Ono T, Watanabe Y. A simple quantitative bradykinesia test in MPTP-treated mice. Res Commun Chem Pathol Pharmacol 1985;50:435.
22. Harms AS, Cao S, Rowse AL, Thome AD, Li X, Mangieri LR, et al. MHCII is required for α-synuclein-induced activation of microglia, CD4 T cell proliferation, and dopaminergic neurodegeneration. J Neurosci 2013;33:9592–600.
23. Cotel MC, Lenartowicz EM, Natesan S, Modo MM, Cooper JD, Williams SC, et al. Microglial activation in the rat brain following chronic antipsychotic treatment at clinically relevant doses. Eur Neuropsychopharmacol 2015;25:2098–107.
24. Shah VO, Ferguson JE, Hunsaker LA, Deck LM, Vander Jagt DL. Natural products inhibit LPS-induced activation of pro-inflammatory cytokines in peripheral blood mononuclear cells. Nat Prod Res 2010;24:1177–88.
25. Olah M, Biber K, Vinet J, Boddeke HW. Microglia phenotype diversity. CNS Neurol Disord Drug Targets. 2011; 10:108–18.
26. Xia CY, Zhang S, Gao Y, Wang ZZ, Chen NH. Selective modulation of microglia polarization to M2 phenotype for stroke treatment. Int Immunopharmacol. 2015;25:377–82.
27. Choi KM, Kashyap PC, Dutta N, Stoltz GJ, Ordog T, Donohue TS, et al. CD206-positive M2 macrophages that express heme oxygenase-1 protect against diabetic gastroparesis in mice. Gastroenterology. 2010;138:2399–409. 2409.e1
28. Bernardo ME, Fibbe WE. Mesenchymal stromal cells: sensors and switchers of inflammation. Cell Stem Cell. 2013;13:392–402.
29. Hoban DB, Connaughton E, Connaughton C, Hogan G, Thornton C, Mulcahy P, et al. Further characterisation of the LPS model of Parkinson's disease: a comparison of intra-nigral and intra-striatal lipopolysaccharide administration on motor function, microgliosis and nigrostriatal neurodegeneration in the rat. Brain Behav Immun. 2013;27:91–100.
30. Castaño A, Herrera AJ, Cano J, Machado A. Lipopolysaccharide intranigral injection induces inflammatory reaction and damage in nigrostriatal dopaminergic system. J Neurochem. 1998;70:1584–92.
31. Bian P, Ye C, Zheng X, Yang J, Ye W, Wang Y, et al. Mesenchymal stem cells alleviate Japanese encephalitis virus-induced neuroinflammation and mortality. Stem Cell Res Ther. 2017;8:38.
32. He T, An X, Mao HP, Wei X, Chen JH, Guo N, et al. Malnutrition-inflammation score predicts long-term mortality in Chinese PD patients. Clin Nephrol. 2013;79:477–83.
33. Ayton S, George JL, Adlard PA, Bush AI, Cherny RA, Finkelstein DI. The effect of dopamine on MPTP-induced rotarod disability. Neurosci Lett. 2013;543:105–9.
34. Dunnett SB, Torres EM, Annett LE. A lateralised grip strength test to evaluate unilateral nigrostriatal lesions in rats. Neurosci Lett. 1998;246:1–4.
35. Matsuura K, Kabuto H, Makino H, Ogawa N. Pole test is a useful method for evaluating the mouse movement disorder caused by striatal dopamine depletion. J Neurosci Methods. 1997;73:45.
36. Mcgeer PL, Mcgeer EG. Glial cell reactions in neurodegenerative diseases: pathophysiology and therapeutic interventions. Alzheimer Dis Assoc Disord. 1998;12 Suppl 2:S1–6.
37. Orihuela R, Mcpherson CA, Harry GJ. Microglial M1/M2 polarization and metabolic states. Br J Pharmacol 2015;173:649–65.
38. Liu Q, Zhang Y, Liu S, et al. Cathepsin C promotes microglia M1 polarization and aggravates neuroinflammation via activation of Ca^{2+}-dependent PKC/p38 MAPK/NF-κB pathway. J Neuroinflammation. 2019;16:10.
39. Benakis C, Garciabonilla L, Iadecola C, Anrather J. The role of microglia and myeloid immune cells in acute cerebral ischemia. Front Cell Neurosci. 2015;8:461.